

CLC \_\_\_\_\_

Number \_\_\_\_\_

UDC \_\_\_\_\_

Available for reference  Yes  No



# Undergraduate Thesis

**Thesis Title:**Classifications and visualization for the behavior of eigenstates in gapless quantum mechanical systems

**Student Name:** Chenlu Huang

**Student ID:** 11910935

**Department:** Department of Mathematics

**Program:** Mathematics and Applied Mathematics

**Thesis Advisor:** Yifei Zhu

Date: May 29, 2024

分类号 \_\_\_\_\_

编号 \_\_\_\_\_

U D C \_\_\_\_\_

密级 \_\_\_\_\_



南方科技大学  
SOUTHERN UNIVERSITY OF SCIENCE AND TECHNOLOGY

# 本科生毕业设计（论文）

题 目： 无隙量子力学系统中本征态行为的  
分类和可视化

姓 名： 黄晨露

学 号： 11910935

系 别： 数学系

专 业： 数学与应用数学

指导教师： 朱一飞

2024 年 5 月 29 日

# Classifications and visualization for the behavior of eigenstates in gapless quantum mechanical systems

Chenlu Huang

(Department of Mathematics Tutor: Yifei Zhu)

**[ABSTRACT]:** The swallowtail catastrophe naturally exists in non-Hermitian systems with both parity-time and pseudo-Hermitian symmetries, revealing transitions among diverse topological singularities. In this thesis, we aim to figure out how eigenvectors behave while changing the parameters. Firstly, we will give some properties of a single swallowtail, whose geometric structure often arises in non-Hermitian systems in a more complicated way. Additionally, we will show detailed calculation process for the evolution of eigenvectors by giving 2-band Hamiltonian as example. Then, we will do similar calculation for a given 3-band non-Hermitian Hamiltonian. Firstly, we will show the stratified parameter space with the dimension of characteristic subspace on the discriminant surface. Based on this, we will calculate several non-trivial loops and illustrate how eigenvectors behave. Moreover, we will show some ideas of further work.

**[Key words]:** Swallowtail; Non-Hermitian Hamiltonian; Singularities; Evolution of eigenvectors

**[摘要]:** 燕尾突变自然存在于具有宇称时间和伪厄米对称性的非厄米系统中，揭示了不同拓扑奇点之间的状态转换。在这篇论文中，我们的目标是找出本征态随参数改变时的演化规律。首先，我们将介绍单个燕尾模型的一些几何性质，它的很多几何结构在非厄米系统的参数空间中经常以更复杂的方式出现。此外，我们将以二能带的哈密顿量为例子，展示我们计算特征向量演化行为的具体过程与方法。同时，二能带系统中特征向量的演化规律也会出现在三能带的一些环路中，这就为我们计算更复杂的情况提供了参考与灵感。接下来，因为三能带非厄米系统的参数空间具有比较复杂的结构，但不同系统之间依然有很多相似之处，所以我们将只对一个三能带的非厄米哈密顿量进行类似的计算。首先，我们将给出对应的分层参数空间，以及判别面上特征子空间维数的情况。基于参数空间的几何结构，我们将计算几个非平凡的环路，用可视化的方  
法说明特征向量的演化规律，并且对这些环路的类型进行初步分类。在最后，我们还将基于现有的结果展示一些进一步的研究想法。

**[关键词]:** 燕尾模型；非厄米哈密顿量；奇点；特征向量的演化规律

# Table of Content

<b>1. Background and introduction</b> . . . . .	<b>1</b>
1.1 Motivation . . . . .	1
1.2 Overview of recent research . . . . .	2
1.3 Introduction of this thesis . . . . .	2
<b>2. Swallowtail</b> . . . . .	<b>3</b>
2.1 Discriminant surfaces . . . . .	3
2.2 Stratified parameter space . . . . .	6
<b>3. 2-band Hamiltonian</b> . . . . .	<b>11</b>
3.1 Hermitian Hamiltonian . . . . .	12
3.2 Non-Hermitian Hamiltonian . . . . .	14
<b>4. Loops in 3-band non-Hermitian Hamiltonian systems</b> . . . . .	<b>17</b>
4.1 A method for reduction . . . . .	17
4.2 Root structure of the parameter space . . . . .	18
4.3 Loops around singularities . . . . .	20
4.4 Loops intersecting with discriminant surface . . . . .	25
<b>5. Further work</b> . . . . .	<b>28</b>
<b>References</b> . . . . .	<b>31</b>
<b>Appendix</b> . . . . .	<b>32</b>
<b>Acknowledgements</b> . . . . .	<b>35</b>

# 1. Background and introduction

## 1.1 Motivation

To describe a physical system, we always use some parameters, such as the temperature and pressure. These parameters can change, and form parameter space. In this thesis, we consider non-Hermitian Hamiltonian matrix with real parameters preserving two symmetries:<sup>[1]</sup>

$$\eta H \eta^{-1} = H^\dagger, [H, PT] = 0 \text{ where } \eta = \begin{pmatrix} 1 & 0 \\ 0 & -I_{n-1} \end{pmatrix}.$$

Here are some examples for such  $H$ :

$$\begin{pmatrix} 1 & f_1 & f_2 \\ -f_1 & -1 & f_3 \\ -f_2 & f_3 & -1 \end{pmatrix}, \begin{pmatrix} 1 - f_1 - f_2 & f_1 & f_2 \\ -f_1 & f_1 - f_3 & f_3 \\ -f_2 & f_3 & f_2 - f_3 \end{pmatrix}, \begin{pmatrix} f_1 f_2 & f_1 & f_2 \\ -f_1 & f_1 & f_3 \\ -f_2 & f_3 & f_2 \end{pmatrix}.$$

In general, the entries of Hamiltonian matrix can be written as polynomials of some relative parameters. Given values of parameters, there will be some energy bands, which are related to eigenvalues in mathematics. When the eigenvalues are distinct, these energy bands are gapped. However, for some singular points, two eigenvalues will degenerate (see Figure 1). Then, the corresponding two energy bands become gapless. If we consider more about the evolutions of the corresponding eigenvectors, then some non-trivial evolutions will arise due to the singularities.

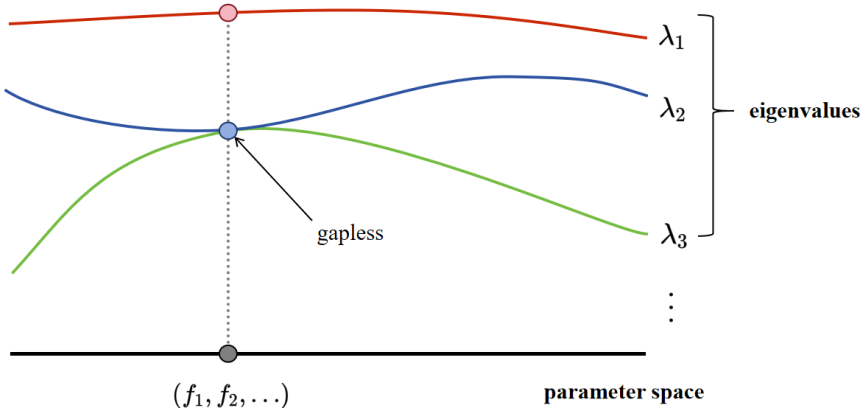


**Figure 1** Gapless Hamiltonian

## 1.2 Overview of recent research

Recently, Prof. Yifei Zhu, in cooperation with Hongwei Jia et al. from the Hong Kong University of Science and Technology, have made a significant progress in studying non-Hermitian systems. They discovered that the swallowtail catastrophe naturally existed in non-Hermitian systems with both parity-time and pseudo-Hermitian symmetries, revealing transitions among diverse topological singularities. The topological structure of the singular spaces involved is extremely rich and intricate, and detailed visualization of these systems under adiabatic evolution has been highly desirable for solving related classification problems.<sup>[1]</sup>

## 1.3 Introduction of this thesis

Our main work will be shown in section 4, but before that we will introduce some simple structures and methods first.

In section 2, we introduce some geometric structure of a single swallowtail, including properties of its discriminant surface and stratified space. In section 3, we show detailed process to calculate the behavior of eigenvectors by giving two examples of Hermitian Hamiltonian and non-Hermitian Hamiltonian respectively.

In section 4, we aim to figure out the behavior of eigenvectors along loops in parameter space. In section 4.1, we introduce an efficient method to figure out the evolution of an n-dimensional ( $n \geq 3$ ) vectors by only figuring out the image of a function. This method offers reduction by focusing on the non-constant part of eigenvectors. In section 4.2, we will give the root structure of a non-Hermitian Hamiltonian. In section 4.3, we calculate two loops around singularities. In section 4.4, we calculate three loops intersecting with discriminant surface. Both in section 4.3 and section 4.4, we mainly show how the directions of eigenvectors change by giving the visualisations for their eigenvector bundles.

In section 5, we will introduce some possible further work, based on the results in section 4.

## 2. Swallowtail

The singularity of a single swallowtail arises in the discriminant surface of

$$f(t) = t^4 + xt^2 + yt + z. \quad (1)$$

where  $x, y, z \in \mathbb{R}$ .

### 2.1 Discriminant surfaces

For every polynomial  $f(t)$  that can be written in the form as equation (1), its coefficients correspond to a point  $(x,y,z)$  in  $\mathbb{R}^3$ . Conversely, for each point  $(x,y,z)$  in  $\mathbb{R}^3$ , it also corresponds to a monic polynomial  $f(t) = t^4 + xt^2 + yt + z$  with real coefficients. Therefore, there exists a bijection between the set  $\{f(t) : f(t) = t^4 + xt^2 + yt + z, (x, y, z) \in \mathbb{R}^3\}$  and  $\mathbb{R}^3$ .

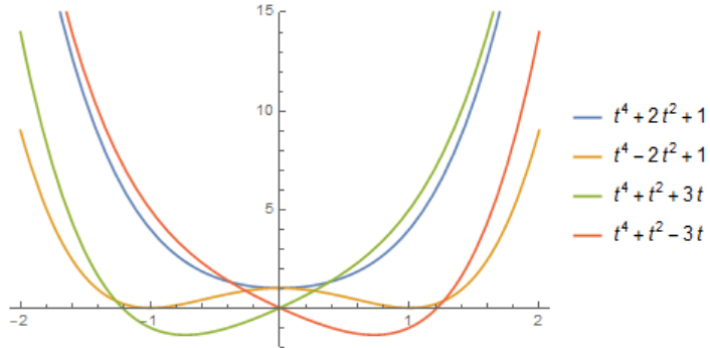


**Figure 2 Polynomials**  $f(t) = t^4 + xt^2 + yt + z$

See Figure 2, when  $(x,y,z)$  varies in  $\mathbb{R}^3$ , the number of real roots and the signs of roots will change. So, we hope to find the root structure of  $f(t)$  in its coefficient space  $\mathbb{R}^3$ . With this hope, we first consider the points where polynomial has repeated roots.

**Definition 2.1** Let  $f(t)$  be a monic polynomial of degree  $n$ . Over  $\mathbb{C}$ ,  $f(t)$  can have  $n$  roots, namely  $t_1, t_2, \dots, t_n$ .

$$f(t) = t^n + \sum_{i=0}^{n-1} a_i t^i = \prod_{i=1}^n (t - t_i) \quad (2)$$

Then, the discriminant  $\Delta$  is

$$\Delta := \prod_{i < j} (t_j - t_i)^2. \quad (3)$$

**Remark 2.2**  $\Delta$  is a polynomial in the coefficients  $a_i (0 \leq i \leq n - 1)$ .

In particular, the discriminant surface of  $f(t) = t^4 + xt^2 + yt + z$  is given by  $\Delta(x, y, z) = 0$ , where repeated roots arise. We will show some properties of this discriminant surface first. Notice that  $f(t)$  has a zero with multiplicity at least 2  $\Leftrightarrow \gcd(f, f') \neq 1 \Leftrightarrow$  there exists  $\tau \in \mathbb{C}$  such that  $f(\tau) = f'(\tau)' = 0$ , which gives equations

$$\begin{cases} \tau^4 + x\tau^2 + y\tau + z = 0 \\ 4\tau^3 + 2x\tau + y = 0 \end{cases} \quad (4)$$

Take  $x$  and  $\tau$  as independent variables. Then, we can solve  $y, z$

$$\begin{cases} y = -\tau^4 - 2x\tau \\ z = 3\tau^4 + x\tau^2 \end{cases} \quad (5)$$

Therefore, the discriminant surface can be parameterized by  $x$  and  $\tau$

$$\begin{pmatrix} x \\ y \\ z \end{pmatrix} = \begin{pmatrix} 0 \\ -4\tau^2 \\ 3\tau^4 \end{pmatrix} + x \begin{pmatrix} 1 \\ -2\tau \\ \tau^2 \end{pmatrix} \quad (6)$$

for all  $x \in \mathbb{R}$  and some  $\tau \in \mathbb{C}$  such that  $y, z \in \mathbb{R}$ .

**Proposition 2.3** The discriminant surface of  $f(t) = t^4 + xt^2 + yt + z$  is a ruled surface with an isolated curve attached at the origin.

*Proof.* To prove this proposition, we consider two cases:  $\tau \in \mathbb{R}$  and  $\tau \in \mathbb{C}$  in the parameterization (6).

For all  $\tau \in \mathbb{R}$ ,  $y$  and  $z$  are already in  $\mathbb{R}$ , and therefore the parameterization (4) is clearly a union of lines in  $\mathbb{R}^3$ , and therefore is a ruled surface. (see Figure 3)

For  $\tau \notin \mathbb{R}$  as a zero of  $f(t)$ , write  $\tau = a + bi$ , where  $a, b \in \mathbb{R}$  and  $b \neq 0$ . Then,  $\bar{\tau} = a - bi$  is also a zero of  $f(t)$  for real coefficient  $x, y, z$ , because

$$f(\bar{\tau}) = \bar{\tau}^4 + x\bar{\tau}^2 + y\bar{\tau} + z = \overline{\tau^4 + x\tau^2 + y\tau + z} = 0.$$

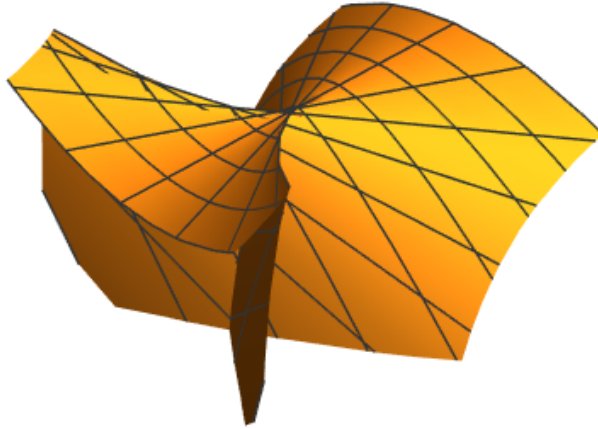


**Figure 3 Ruled surface**

So, if  $\tau \notin \mathbb{R}$  is a zero with multiplicity at least 2, then  $\bar{\tau}$  is a distinct zero also with multiplicity at least 2. Therefore,  $\tau, \bar{\tau}, \bar{\tau}$  are all zeros of  $f(t)$  with none of them is real. Then, we can write  $f(t) = (t - \tau)^2(t - \bar{\tau})^2 = [(t - a)^2 + b^2]^2$ . Since it must have the form as  $f(t) = t^4 + xt^2 + yt + z$  (i.e. the coefficient of  $t^3$  is 0), then  $a=0$  and  $f(t) = (t^2 + b^2)^2 = t^4 + 2b^2t^2 + b^4$ . Therefore, all points  $(x,y,z)$  such that  $f(t)$  has two double complex roots form an isolated curve parameterized by  $b$

$$\begin{cases} x = 2b^2 \\ y = 0 \\ z = b^4 \end{cases}, b \in \mathbb{R} \quad (7)$$

Eliminating the parameter  $b$ , we obtain

$$\begin{cases} x^2 = 4z \\ y = 0 \end{cases}, (x > 0) \quad (8)$$

which is a half of parabola.

Since  $f(t)$  cannot have real roots along this curve, then this curve does not intersect with the ruled surface. However, take  $x \rightarrow 0$ ,  $(x, y, z) \rightarrow (0, 0, 0)$ . So, they are connected at

the origin. We complete the proof.

Actually, we have a similar proposition for the discriminant surface of a kind of polynomials at any degree  $n$  ( $n \geq 3$ ).

**Proposition 2.4** The discriminant surface  $S \subseteq k^3$  of

$$P(x, y, z, t) = f(t) + xg(t) + yt + z \in k[x, y, z, t]$$

is a ruled surface, where  $k$  is algebraic closed and  $f, g \in k[t]$  satisfying

- (1)  $f$  is monic;
- (2)  $n = \deg(f) > \deg(g) > 1$ ;
- (3)  $\frac{df}{dt} \neq 0$  and  $\frac{d^2g}{dt^2} \neq 0$ ;
- (4)  $\text{char}(k) \neq 2, 3, 5$ .<sup>[2]</sup>

## 2.2 Stratified parameter space

Next, we will shift our attention from the surface to the whole space. Before giving a specific structure, we will give a brief explanation of the word “stratified”.

An  $n$ -dimensional topological stratification of  $X$  is a filtration

$$\emptyset = X_{-1} \subset X_0 \subset X_1 \cdots \subset X_n = X.$$

We call  $X$  a stratified space, and the  $i$ -dimensional stratum of  $X$  is the space  $X_i \setminus X_{i-1}$ .

Saying roughly, if a topological space is equipped with a partition into smooth manifolds, then it is called a stratified space.<sup>[3]</sup>

If we consider the three real coefficients  $x, y, z$  as parameters, then the parameter space  $\mathbb{R}^3$  is a stratified parameter space. By the continuity of the natural map from  $(x, y, z)$  to four roots in  $\mathbb{C}$ , the discriminant surface split the coefficient space into some path connected components, each of which stands for one situation of roots. Therefore, we can describe the situations of roots in a geometric way, which we call “root structure”.

For polynomials of degree 4, there are 5 possible situations for the number of the repeated roots (see Table 1). Here, same numbers mean repeated roots and different numbers

mean distinct roots. For example, type 1111 means there is a quadruple root, and type 1234 means four distinct roots.

**Table 1 Types of roots**

1234	four distinct roots
1123	a double root and two distinct roots
1122	two double roots
1112	a triple root and a distinct root
1111	a quadruple root

Let  $S(\text{type})$  denote all the points in the parameter space where the corresponding type arises. Take  $X = X_3 = \mathbb{R}^3$ ,  $X_3 \setminus X_2 = S(1234)$ ,  $X_2 \setminus X_1 = S(1123)$ ,  $X_1 \setminus X_0 = S(1122) \cup S(1112)$  and  $X_0 = S(1111)$ . Then, we will show that this is a stratification of the parameter space  $X = \mathbb{R}^3$ . Here,  $X_2 \setminus X_1$  are pieces of surfaces; and  $X_1 \setminus X_0$  are several special curves.

To give more specific root structure, we use r to denote a real root and use c to denote a complex root with nonzero imaginary part. Then, there are different finer types for 1234,1123 and 1122.

**Table 2 Finer types of roots**

1234	rrrr rrcc cccc
1123	rrrr rrcc
1122	rrrr cccc

For  $X_2$ , it is the discriminant surface containing types of roots: 1123,1122,1112 and 1111. Also, it splits  $S(1234)$  into three different path connected components with different finer types: rrrr,rrcc and cccc. (see Figure 4)

For  $X_1$ , it is some special curves on the discriminant surface intersecting at a point.

Here, we will give their parametrizations for different finer types.

- Type 1122(cccc): two double complex roots

Recall equation (8), it is the curve

$$\begin{cases} x^2 = 4z \\ y = 0 \end{cases}, (x > 0) \quad (9)$$

- Type 1122(rrrr): two double real roots

Suppose  $f(t) = (t - a)^2(t - b)^2$ . Expanding  $f(t)$ , then we have  $f(t) = t^4 - 2(a + b)t^3 + (a^2 + 4ab + b^2)t^2 - 2ab(a + b)t + a^2b^2$  with  $a, b \in \mathbb{R}$ . Since  $f(t)$  has the form  $f(t) = t^4 + xt^2 + yt + z$ , then

$$\begin{cases} 0 = 2(a + b) \\ x = a^2 + 4ab + b^2 \\ y = -2ab(a + b) \\ z = a^2b^2 \end{cases} \quad (10)$$

Eliminating  $b$  by  $2(a + b) = 0$ , we obtain a parametrization for the curve

$$\begin{cases} x = -2a^2 \\ y = 0 \\ z = a^4 \end{cases}, a \in \mathbb{R} \quad (11)$$

So, the curve is

$$\begin{cases} x^2 = 4z \\ y = 0 \end{cases}, (x < 0) \quad (12)$$

which is another half of the parabola.

- Type 1112(rrrr): triple root

Suppose  $f(t) = (t - a)^3(t - b)$  with  $a \neq b$ . Similarly, we can obtain the parameterization of it

$$\begin{cases} x = -6a^2 \\ y = 8a^3 \\ z = -3a^4 \end{cases}, a \in \mathbb{R}, a \neq 0 \quad (13)$$

If we modify the type 1112 by comparing the triple root and the fourth root (see Table3), then the corresponding curves have same expressions as equation(13) with  $a<0$  and  $a>0$  respectively.

**Table 3 Finer types of roots for triple roots**

1112	The triple root is less than the fourth root.
1222	The triple root is larger than the fourth root.

Finally, for  $X_0$ , it is the origin  $(0,0,0)$ , where four different path connected components of  $X_1 \setminus X_0$  (i.e. the four special curves above) meet. So, we call it as meeting point.

The stratified parameter space gives the root structure. (see Figure 4)

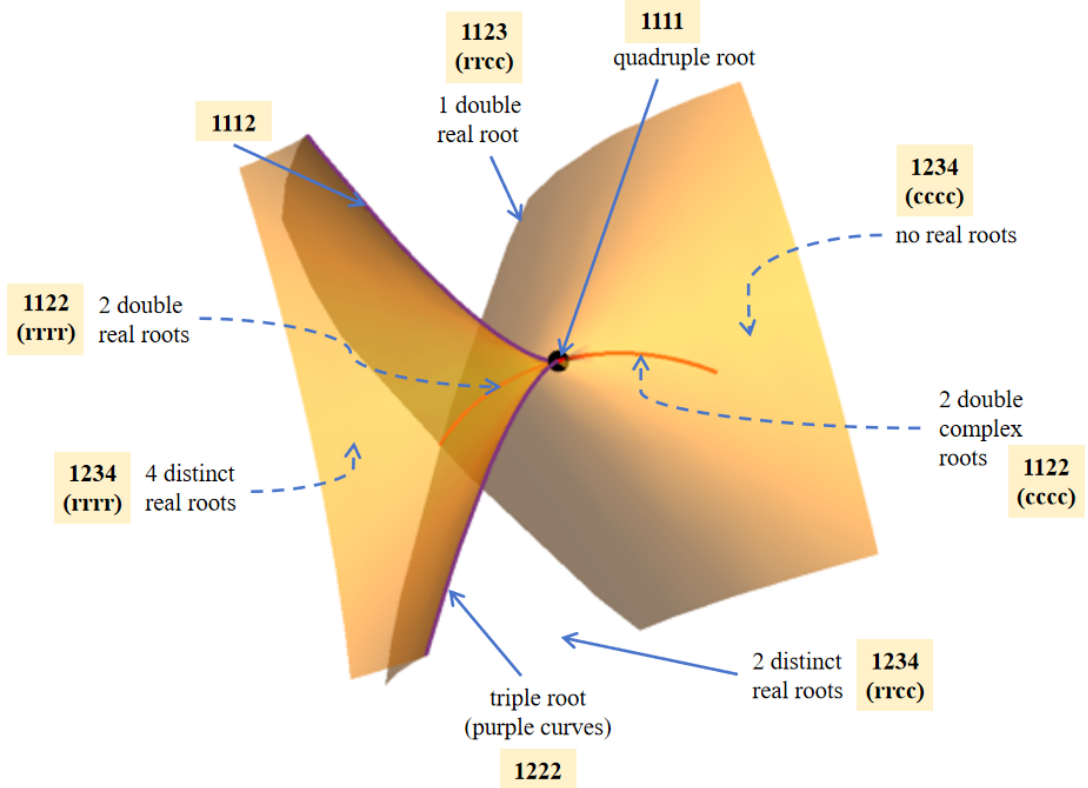


**Figure 4 Root structure**

For a given non-Hermitian Hamiltonian matrix  $H[f_1, f_2, f_3]$  with parameters  $f_1, f_2, f_3 \in \mathbb{R}$ , we can also obtain a discriminant surface in  $\mathbb{R}^3$  by its characteristic polynomial  $f(\lambda) = |H - \lambda I|$ . The discriminant surfaces of the 3 non-Hermitian Hamiltonian matrices mentioned in section1.1 can be seen in Figure 5 respectively.

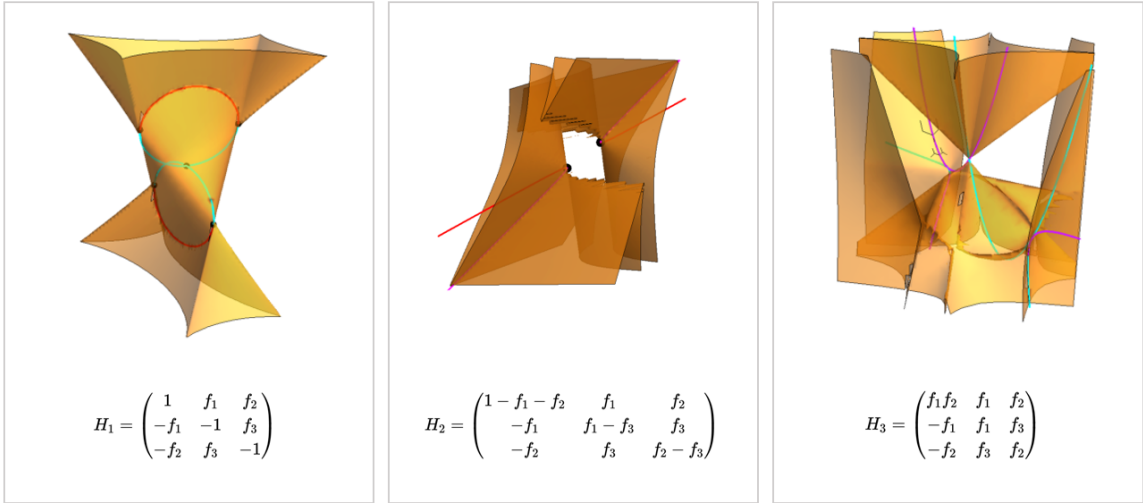


**Figure 5 Discriminant surfaces**

Although multiplicities of eigenvalues are different from the situations of the single swallowtail, these discriminant surfaces have similar geometric structure locally. The first discriminant surface can be think of as four swallowtails connected. The second is two separated swallowtails. The third discriminant surface is four swallowtails connected in a more complicated way with some other geometric structures such as cones.

Similar to the single swallowtail, the corresponding root structures can be given. (Here is an example for  $H_1$  to be seen in section3.2.) For the convenience of mentioning the similar geometric structures in Figure 6 later, we give notations as the Table 4.

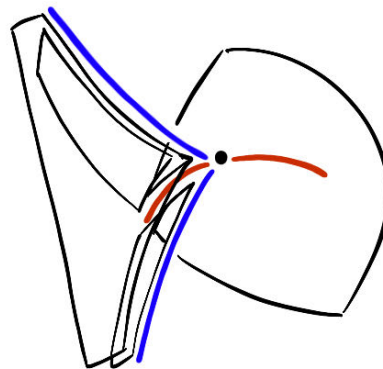


**Figure 6 Stratified parameter space**

**Table 4** Notations for exceptional surfaces, lines and points<sup>[1]</sup>

Notations	Types of roots in a single swallowtail	Geometric features in Figure 6
ES	1123	surfaces with black “edges”
NIL	1122(rrrr)	the red curve where two ESs meet
NL	1122(cccc)	the isolated red curve
EL	1112 or 1222	the blue curves
MP	1111	the black meeting point of the above curves

### 3. 2-band Hamiltonian

After figuring out the structure of the parameter space, we can consider the evolutions of the corresponding eigenvectors (or “eigenstates” in physics) along some loops.

At each point in the parameter space, the eigenvectors can change continuously. However, there is some difference between the real eigenvectors and the complex eigenvectors (with nonzero imaginary part).

For real eigenvalues, the corresponding eigenvectors are real. Moreover, there are only two corresponding unit eigenvectors, namely  $v$  and  $-v$ , for a given eigenvalue  $\lambda$  with multiplicity 1. Notice that the map  $v \rightarrow -v$  is discontinuous but the eigenvalues and the corresponding eigenvectors are change continuously. Therefore, if we fixed the initial direction of an eigenvector, then the final direction is unique as long as the eigenvalue keep real along the loop.

Unlike this, for a complex eigenvalue, it has infinitely many corresponding unit complex eigenvectors. Moreover, by multiplying a complex eigenvector by  $e^{i\theta(t)}$ , we can rotate it to any direction we want within a path continuously whenever  $\theta(t)$  is a continuous function.

In general, we only consider conjugate (or reversely conjugate) eigenvectors for conjugate eigenvalues. When we take the Hermitian angle to describe the relative position of two conjugate (or reversely conjugate) eigenvectors, the result is independent of the expressions we use for eigenvectors. Unfortunately, we still cannot have a unique solution in mathemat-

ics for the final direction of an eigenvector, which is an unsolved problem in this thesis. In section 3-4, we just give some expressions for eigenvectors which are consistent with the result of physical experiments.

In this section, we will give examples of 2-band Hermitian Hamiltonian and non-Hermitian Hamiltonian to show detailed calculation process for the evolution of eigenvectors, which will provide inspiration for 3-band cases.

### 3.1 Hermitian Hamiltonian

**Example 3.1** Take

$$H = \begin{pmatrix} f_3 & f_1 \\ f_1 & -f_3 \end{pmatrix}$$

Its characteristic polynomial is  $f(\lambda) = |H - \lambda I| = \lambda^2 - f_1^2 - f_3^2$ , where  $I$  is the  $2 \times 2$  identity matrix. So, the parameter space  $\mathbb{R}^2$  has only one singularity at the origin. Write two eigenvalues  $\lambda_+ = \sqrt{f_1^2 + f_3^2}$  and  $\lambda_- = -\sqrt{f_1^2 + f_3^2}$ . Then, the corresponding eigenvectors are

$$v_+ = \begin{pmatrix} f_3 + \sqrt{f_1^2 + f_3^2} \\ f_1 \end{pmatrix}, v_- = \begin{pmatrix} f_3 - \sqrt{f_1^2 + f_3^2} \\ f_1 \end{pmatrix}.$$

We can see that eigenvalues and eigenvectors are real. Additionally, the eigenvectors corresponding to distinct eigenvalues are orthogonal to each other. Although this conclusion can be obtained without calculation because  $H$  is a real symmetric matrix, with concrete expressions of eigenvectors we can go further.

Now, we can consider a loop around the singularity (i.e. the origin)

$$\begin{cases} f_1 = \cos t \\ f_3 = \sin t \end{cases}, t \in [0, 2\pi],$$

The eigenvectors can be expressed as

$$v_+ = \begin{pmatrix} \sin t + 1 \\ \cos t \end{pmatrix}, v_- = \begin{pmatrix} \sin t - 1 \\ \cos t \end{pmatrix}.$$

Then, we normalize  $v_+$  and  $v_-$ , and plot their first and second components respectively. (see Figure 7)

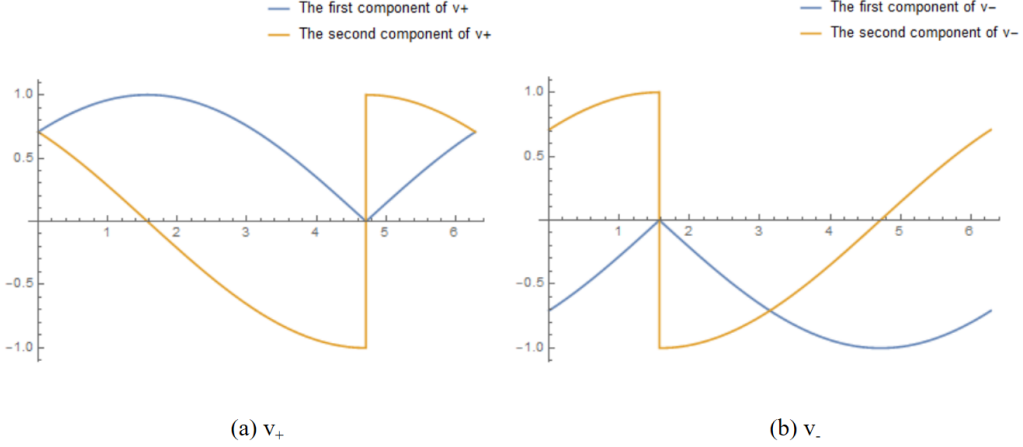


**Figure 7 The first and second components of  $v_+$  and  $v_-$**

Notice that the discontinuities arise at  $t = \frac{3\pi}{2}$  and  $t = \frac{\pi}{2}$  respectively. These discontinuities can be seen as  $v$  changes to  $-v$  at these points. So we can take proper signs to ensure the continuity of their change.

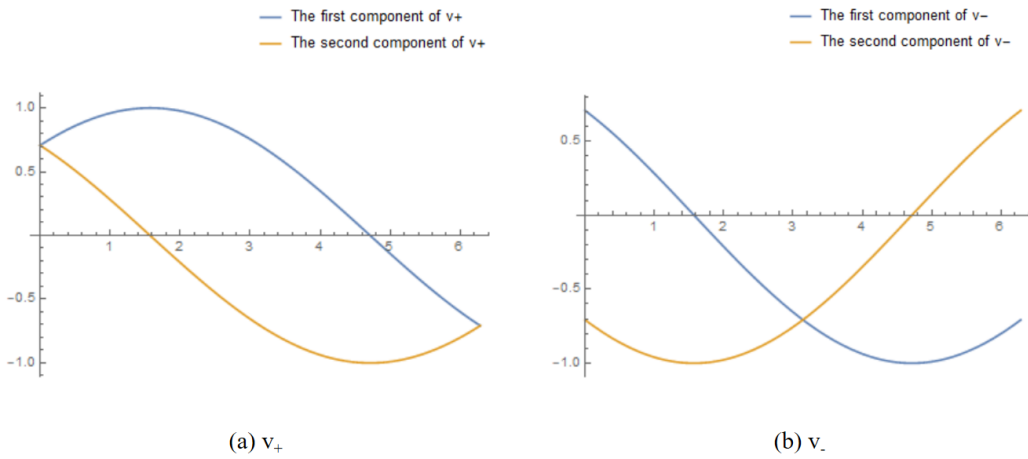


**Figure 8 The first and second components of  $v_+$  and  $v_-$**

To be specific, take

$$v_+ = \frac{1}{\sqrt{(\sin t + 1)^2 + \cos^2 t}} \begin{pmatrix} \sin t + 1 \\ \cos t \end{pmatrix}, t \in [0, \frac{3\pi}{2})$$

$$v_+ = -\frac{1}{\sqrt{(\sin t + 1)^2 + \cos^2 t}} \begin{pmatrix} \sin t + 1 \\ \cos t \end{pmatrix}, t \in [\frac{3\pi}{2}, 2\pi]$$

and

$$v_- = \frac{1}{\sqrt{(\sin t - 1)^2 + \cos^2 t}} \begin{pmatrix} \sin t - 1 \\ \cos t \end{pmatrix}, t \in [0, \frac{\pi}{2})$$

$$v_- = -\frac{1}{\sqrt{(\sin t - 1)^2 + \cos^2 t}} \begin{pmatrix} \sin t - 1 \\ \cos t \end{pmatrix}, t \in [\frac{\pi}{2}, 2\pi].$$

Then, the Figure 8 shows that the eigenvectors change continuously to their opposite directions from  $t = 0$  to  $t = 2\pi$ .

Moreover, using these continuous expressions of  $v_+$  and  $v_-$ , we can obtain the corresponding eigenvector bundles from  $t = 0$  to  $t = 2\pi$ . The two bundles are half of two Möbius bands orthogonal to each other everywhere.

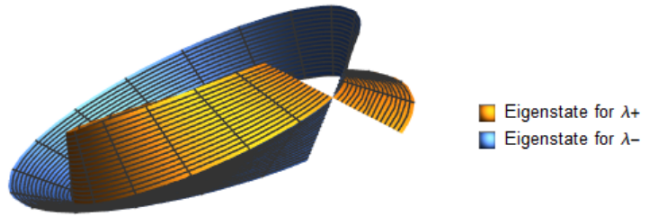


**Figure 9**  $t$  varies from 0 to  $2\pi$

If  $t$  varies from 0 to  $4\pi$ , then two eigenvectors are back to the initial situations, and the bundles could be two complete Möbius bands.

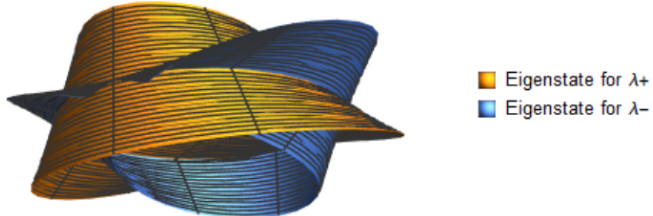


**Figure 10**  $t$  varies from 0 to  $4\pi$

We will see similar results in a 3-band system later.

### 3.2 Non-Hermitian Hamiltonian

**Example 3.2** Take

$$H = \begin{pmatrix} f_3 & f_1 \\ -f_1 & -f_3 \end{pmatrix}$$

Its characteristic polynomial is  $f(\lambda) = |H - \lambda I| = \lambda^2 + f_1^2 - f_3^2$ . Two eigenvalues are

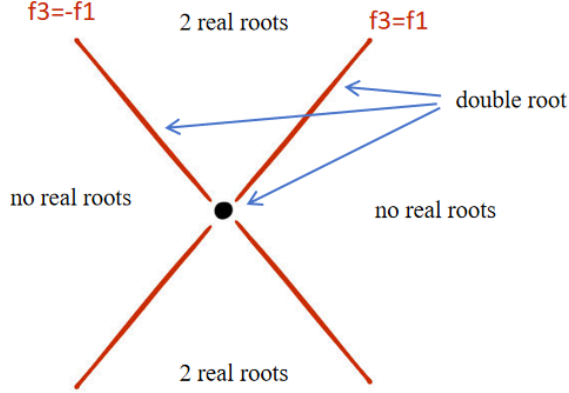


**Figure 11** Stratified parameter space of  $H$

$\lambda_+ = \sqrt{f_3^2 - f_1^2}$  and  $\lambda_- = -\sqrt{f_3^2 - f_1^2}$ . When  $f_1 = f_3$  or  $f_1 = -f_3$ ,  $f(\lambda)$  has a double real root. When  $|f_1| > |f_3|$ , there are two distinct real eigenvalues. When  $|f_1| < |f_3|$ , there are two distinct complex eigenvalues with nonzero imaginary part. (see Figure 11) This root structure is more complicated than the 2-band Hermitian case.

Take the corresponding eigenvectors

$$v_+ = \begin{pmatrix} f_3 + \sqrt{f_3^2 - f_1^2} \\ -f_1 \end{pmatrix}, v_- = \begin{pmatrix} f_3 - \sqrt{f_3^2 - f_1^2} \\ f_1 \end{pmatrix}.$$

Consider a loop containing the origin

$$\begin{cases} f_1 = \cos t \\ f_3 = \sin t \end{cases}, t \in [0, 2\pi],$$

$\lambda_+$  and  $\lambda_-$  are real when  $t \in [\frac{\pi}{4}, \frac{3\pi}{4}] \cup [\frac{5\pi}{4}, \frac{7\pi}{4}]$ .

The eigenvectors along this loop can be expressed as

$$v_+ = \begin{pmatrix} \sin t + \sqrt{-\cos 2t} \\ -\cos t \end{pmatrix}, v_- = \begin{pmatrix} \sin t - \sqrt{-\cos 2t} \\ \cos t \end{pmatrix}.$$

Let

$$a(t) = \frac{\sin t}{\|v_+\|}$$

$$b(t) = -\frac{\cos t}{\|v_+\|}$$

$$c(t) = \frac{|\sqrt{-\cos 2t}|}{\|v_+\|}$$

When  $v_+$  is real, we can write

$$\frac{v_+}{\|v_+\|} = \begin{pmatrix} a(t) + c(t) \\ b(t) \end{pmatrix} \quad (14)$$

When it is complex, we write

$$\frac{v_+}{\|v_+\|} = \begin{pmatrix} a(t) + c(t)i \\ b(t) \end{pmatrix} \quad (15)$$

Then, taking proper signs, we can plot the image of two components of  $v_+$  when it is real and plot  $a(t)$ ,  $b(t)$ ,  $c(t)$  respectively when it is complex. Similarly, we can plot the image of components of  $v_-$ . (see Figure 12)

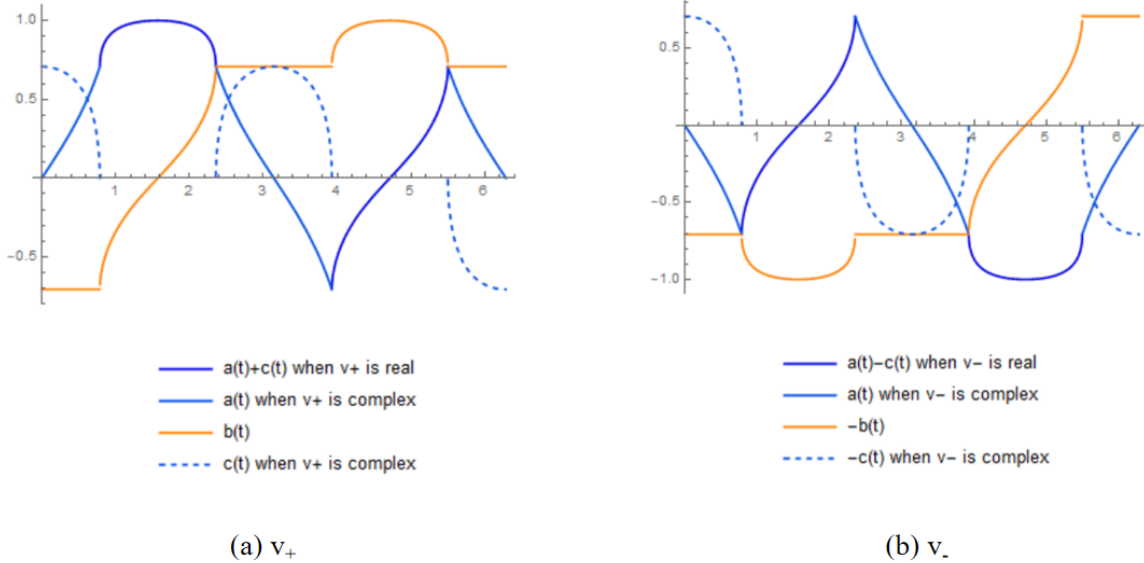


**Figure 12 Image of components of  $v_+$  and  $v_-$**

When  $t$  varies from 0 to  $2\pi$ ,  $v_+$  changes to  $-v_+$  and  $v_-$  changes to  $-v_-$ . Moreover, they are conjugate for  $t \in (\frac{3\pi}{4}, \frac{5\pi}{4})$  and reversely conjugate for  $t \in [0, \frac{\pi}{4}] \cup (\frac{7\pi}{4}, 2\pi]$ .

Therefore, the corresponding eigenvector bundles are also half of Möbius bands, but they are not orthogonal.

## 4. Loops in 3-band non-Hermitian Hamiltonian systems

Although 3-band cases are more complicated, the calculation steps are similar with the 2-band cases. So, in this section, we will skip some calculation steps and only give the expressions of eigenvalues and eigenvectors.

Firstly, we will introduce a quick method to determine whether the eigenvectors change to its opposite direction.

### 4.1 A method for reduction

When calculating how the vectors behave along loops, it is hard to plot vectors in higher dimension. However, when the loops lie in some planes related to the symmetry of the discriminant surface, the explicit expressions of eigenvectors are not so complicated. In this section, we will introduce a method to simplify the calculation in a special situation.

Let  $v$  be a unit vector in  $\mathbb{R}^n$ . If  $v$  can be written in the form

$$v = \begin{bmatrix} v_1 \\ v_2 \\ \vdots \\ f(t) \\ \vdots \\ v_n \end{bmatrix},$$

where  $v_i \in \mathbb{R}$  ( $1 \leq i \leq n$ ) are constant except for  $v_j = f(t) \in \mathbb{R}$  a function for some  $1 \leq j \leq n$ .

Then, the trace of the end point of  $\frac{v}{|v|}$  is contained in a circle  $S^1$ .

Only the trace is not enough. We still need to know how  $v$  rotates along such circle. To ensure that the vector changes continuously, we only need to remove the infinite discontinuity points of  $f(t)$ . (  $f(t)$  cannot have other kinds of discontinuity. )

Let  $N$  denote the plane (or hyperplane) where  $\omega$  in it satisfies

$$\omega = \begin{bmatrix} v_1 \\ v_2 \\ \vdots \\ v_{j-1} \\ 0 \\ v_{j+1} \\ \vdots \\ v_n \end{bmatrix}.$$

To ensure the continuity of the vectors, only one condition need to be required: the point  $a$  which represents the value of  $f(t)$  can pass through the plane  $N$  only when  $f(t)=0$ . Moreover, it is only allowed to move from  $-\infty$  to  $+\infty$  on the same side of  $N$ . So, we can identity two pairs of  $-\infty$  and  $+\infty$ , and then gain an  $S^1$ . Obviously, there exist an homeomorphism between two  $S^1$ . (see Figure 13)

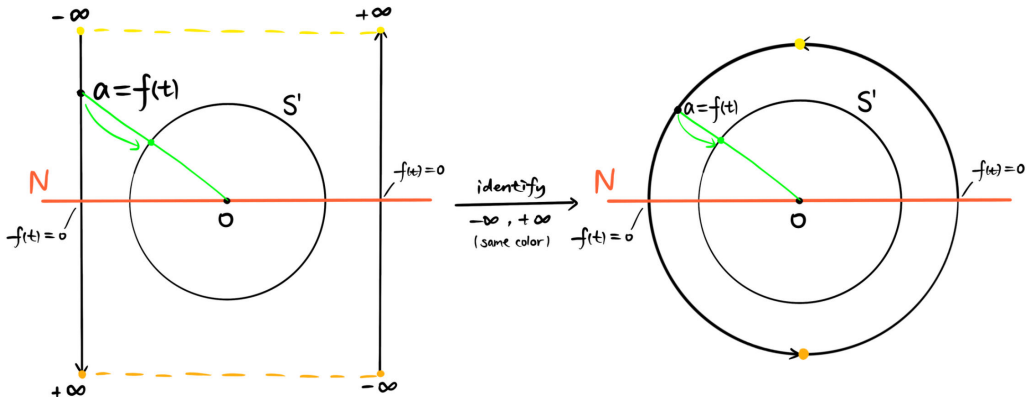


**Figure 13 A method for reduction**

More generally, for functions  $f(t) \in \mathbb{C}$ , the method still works if we use the complex planes instead of axes and consider  $S^2$  instead of  $S^1$ .

## 4.2 Root structure of the parameter space

In section 4, we give examples for the following specific Hamiltonian.

$$H_1 = \begin{pmatrix} 1 & f_1 & f_2 \\ -f_1 & -1 & f_3 \\ -f_2 & f_3 & -1 \end{pmatrix}$$

Before calculating the evolutions of eigenvectors in this parameter space, we need to

give its specific root structure first.

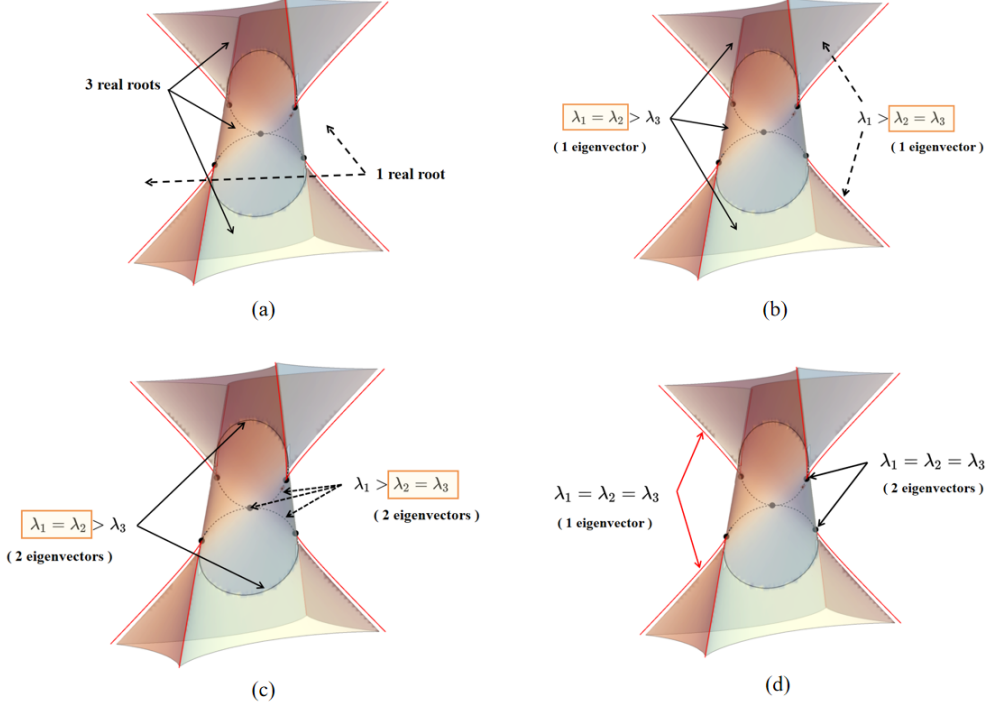


**Figure 14 Root structure of the parameter space**

Let  $h(\lambda) = |H - \lambda I|$  be the characteristic polynomial. Then, solving the equations  $h = h' = h'' = 0$ , we can obtain the ELs. (The explicit expressions of ELs are too complicated to write down, but one parametrization is given in the appendix.) Note that ELs are symmetrical about two planes, namely  $f_1 = f_2$  and  $f_1 = -f_2$ . So, we can find NILs and NILs by solving  $\Delta(f_1, f_2, f_3) = 0$  under conditions  $f_1 = f_2$  and  $f_1 = -f_2$  respectively. Then, we obtain the root structure. Here, we will give more information about the dimension of the characteristic subspace.

Points that are not on the surface are divided into four regions (see Figure 14(a)), three of which have three distinct real roots. Besides, the discriminant surface is divided into several pieces of surfaces, all of which can be classified into three different kinds according to their geometric shapes. The pieces of surface whose shapes are like a triangle has smaller double roots than the third roots. Other pieces of surface has larger double roots than the third roots. Both of these two kinds has 1-dimensional characteristic subspace for the double roots (see Figure 14(b)). Additionally, NILs and NILs here are two orthogonal circles intersecting at

the origin with two isolated arcs perpendicular to each other. Along these two circles, the relationship between the eigenvalues is as shown in the figure and almost all points have 3 distinct eigenvectors except for four meeting points (see Figure 14(c)). Finally, the EL3s are points where triple roots arise with 1-dimensional characteristic subspace (see Figure 14(d)).

- 2NILs and 4 NLs

$$\begin{cases} f_1 = \cos t \\ f_2 = -\cos t \\ f_3 = 1 + \sin t \end{cases}, t \in [0, 2\pi)$$

$$\begin{cases} f_1 = \cos t \\ f_2 = \cos t \\ f_3 = -1 + \sin t \end{cases}, t \in [0, 2\pi)$$

- 5 MPs

$$\left(\frac{2\sqrt{2}}{3}, -\frac{2\sqrt{2}}{3}, \frac{2}{3}\right), \left(-\frac{2\sqrt{2}}{3}, \frac{2\sqrt{2}}{3}, \frac{2}{3}\right), \left(\frac{2\sqrt{2}}{3}, \frac{2\sqrt{2}}{3}, -\frac{2}{3}\right), \left(-\frac{2\sqrt{2}}{3}, -\frac{2\sqrt{2}}{3}, -\frac{2}{3}\right), (0, 0, 0)$$

Notice that it seems to be simpler than the root structure of single swallowtail, because there can only be 1 or 3 real roots for polynomials of degree 3 and there cannot have a pair of double complex roots. However, it still have similar shapes with a single swallowtail. For other non-Hermitian Hamiltonian, their structures are also similar. So, it is considerable to only consider the specific Hamiltonian given before.

With the root structure, it is easier for us to study the behavior of eigenvectors. In the following sections, we only calculate some special loops. However, by the continuity, we can obtain the same evolution for several kinds of loops.

### 4.3 Loops around singularities

In this section, we will calculate two loops around an NL and a MP respectively. (see Figure 15)

**Example 4.1** The first loop (see Figure 15(a)) is given by the following parametrization

$$\alpha_1 : [-\pi, \pi] \longrightarrow \mathbb{R}^3$$

$$\alpha_1 : t \longmapsto (f_1, f_2, f_3)$$

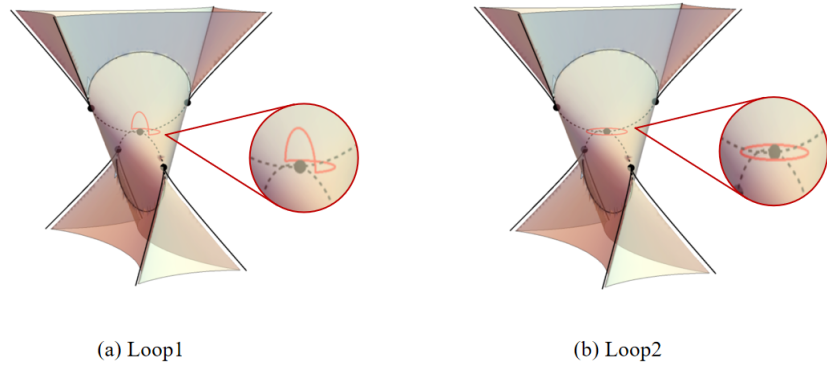


**Figure 15 Two loops around singularities**

$$\begin{cases} f_1 = \frac{1}{2\sqrt{2}} \cos t \\ f_2 = \frac{1}{2\sqrt{2}} \cos t, t \in [-\pi, 0] \\ f_3 = -\frac{1}{2} \sin t \end{cases}$$

For  $t \in [-\pi, 0]$ , the eigenvalues are

$$\begin{aligned}\lambda_1 &= \frac{1}{8}(-2 \sin t + \sqrt{2(29 - 5 \cos 2t + 16 \sin t)}) \\ \lambda_2 &= \frac{1}{8}(-2 \sin t - \sqrt{2(29 - 5 \cos 2t + 16 \sin t)}) \\ \lambda_3 &= -1 + \frac{1}{2} \sin t\end{aligned}$$

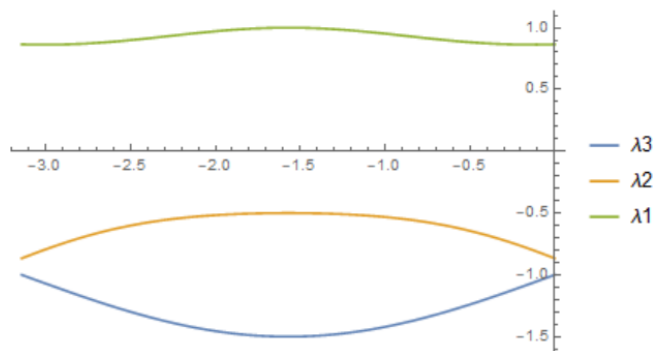


**Figure 16** Eigenvalues for  $t \in [-\pi, 0]$

For  $t \in [0, \pi]$ , the eigenvalues are distinct constants

$$\lambda_1 = \frac{\sqrt{3}}{2}, \lambda_2 = -\frac{\sqrt{3}}{2}, \lambda_3 = -1$$

Since the loop does not intersect with the discriminant surface, then the eigenvalues keep distinct. Moreover, the corresponding three eigenvectors are linearly independent everywhere. So, we can obtain three eigenvector bundles without intersection or exchange, each of which illustrates how the corresponding eigenvector behave along this loop.

For  $t \in [-\pi, 0]$ , the corresponding eigenvectors are

$$v_1 = \begin{pmatrix} 0 \\ -1 \\ 1 \end{pmatrix}$$

$$v_2 = \begin{pmatrix} \frac{1}{2}(-4\sqrt{2} \sec t + \sec t \sqrt{29 - 5 \cos(2t) + 16 \sin t} - \sqrt{2} \tan t) \\ 1 \\ 1 \end{pmatrix}$$

$$v_3 = \begin{pmatrix} \frac{1}{2}(-4\sqrt{2} \sec t - \sec t \sqrt{29 - 5 \cos(2t) + 16 \sin t} - \sqrt{2} \tan t) \\ 1 \\ 1 \end{pmatrix}$$

For  $t \in [0, \pi]$ , the corresponding eigenvectors are

$$v_1 = \begin{pmatrix} 0 \\ -\tan(\frac{\pi}{4} + t) \\ 1 \end{pmatrix}$$

$$v_2 = \begin{pmatrix} -(2 + \sqrt{3}) \csc(\frac{\pi}{4} + t) \\ \cot(\frac{\pi}{4} + t) \\ 1 \end{pmatrix}$$

$$v_3 = \begin{pmatrix} (\sqrt{3} - 2) \csc(\frac{\pi}{4} + t) \\ \cot(\frac{\pi}{4} + t) \\ 1 \end{pmatrix}$$

We can gain three stratified vector bundles along this loop by considering the unit eigenvectors. (see Figure 17)

The first bundle is trivial. The second and the third ones show that eigenvectors  $v_2$  (or  $v_3$ ) rotate to their opposite direction  $-v_2$  (or  $-v_3$ ) from  $t = -\pi$  to  $t = \pi$ . Similar to the 2-band cases, these two bundles can be seen as half of Möbius bands.

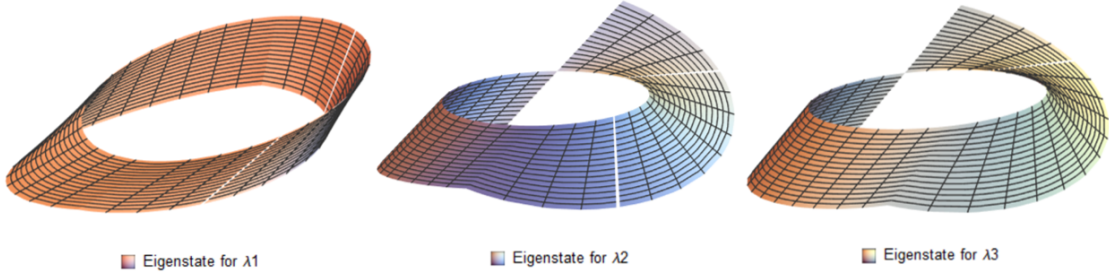


**Figure 17 Eigenvector bundles for loop1**

**Example 4.2** The second loop (see Figure 15(b)) is given by the following parametrization

$$\alpha_2 : [0, 2\pi] \longrightarrow \mathbb{R}^3$$

$$\alpha_2 : t \longmapsto (f_1, f_2, f_3)$$

$$\begin{cases} f_1 = \frac{1}{2} \cos t \\ f_2 = \frac{1}{2} \sin t, t \in [0, 2\pi] \\ f_3 = 0 \end{cases}$$

The eigenvalues are

$$\lambda_1 = \frac{\sqrt{3}}{2}, \lambda_2 = -\frac{\sqrt{3}}{2}, \lambda_3 = -1,$$

and the corresponding eigenvectors are

$$v_1 = \begin{pmatrix} -(2 + \sqrt{3}) \csc t \\ \cot t \\ 1 \end{pmatrix}$$

$$v_2 = \begin{pmatrix} (\sqrt{3} - 2) \csc t \\ \cot t \\ 1 \end{pmatrix}$$

$$v_3 = \begin{pmatrix} 0 \\ -\tan t \\ 1 \end{pmatrix}$$

We can also gain three stratified vector bundles. However, the frame of eigenvectors cannot keep parallel to the three coordinate axes of the loop in this case. More explanation will be given in the following.

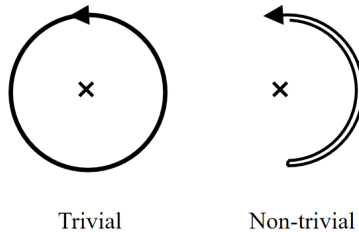


**Figure 18 Two different kinds of behavior of eigenvectors**

We hope to distinguish between the two situations in Figure 18.

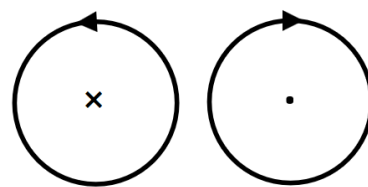


**Figure 19 Offset**

Let  $t$  be the tangent vector of the loop. Let “ $\times$ ” denote that the direction of  $t$  is into the paper, and “ $\cdot$ ” denote that  $t$  is outward the paper. For the non-trivial situation, if the frame of eigenvectors is parallel to the three coordinate axes, then there will exist an offset along the loop, which leads to a trivial bundle. (see Figure 19)

Therefore, we need to modify the frame of eigenvectors here such that the angle between this frame and the Frenet frame of the loop is constant. After this modification, we obtain the following eigenvector bundles. (see Figure 20)

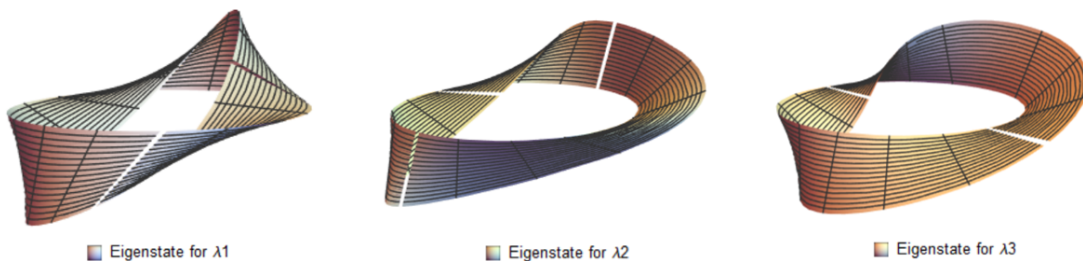


**Figure 20 Eigenvector bundles**

All eigenvectors rotate to their initial position. However, the second and the third bundles are non-trivial with rotation  $\pi$ .

#### 4.4 Loops intersecting with discriminant surface

We can do similar work for other loops which pass through the discriminant surface in the parameter space. (see Figure 21)

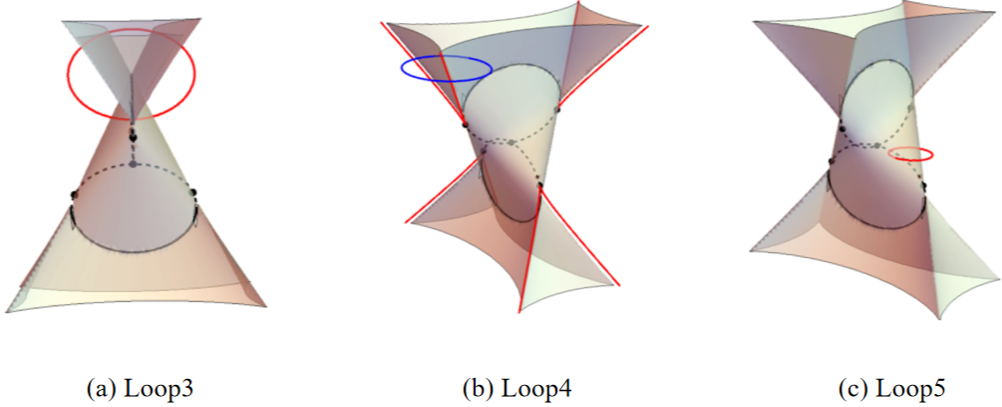


**Figure 21** Three loops intersecting with discriminant surface

**Example 4.3** The third loop (see Figure 21(a)) is parameterized by

$$\alpha_3 : [0, 2\pi] \longrightarrow \mathbb{R}^3$$

$$\alpha_3 : t \longmapsto (f_1, f_2, f_3)$$

$$\begin{cases} f_1 = \cos t \\ f_2 = \cos t \\ f_3 = 2 + \sin t \end{cases}, t \in [0, 2\pi]$$

The eigenvalues are

$$\lambda_1 = \frac{1}{2}(2 + \frac{\sqrt{-7 - 9 \cos 2t}}{\sqrt{2}} + \sin t)$$

$$\lambda_2 = \frac{1}{2}(2 - \frac{\sqrt{-7 - 9 \cos 2t}}{\sqrt{2}} + \sin t)$$

$$\lambda_3 = -3 - \sin t$$

In Figure 22, we only plot the eigenvalues when they are real. We can see that  $\lambda_1$  and  $\lambda_2$  become the same fourth time, which is consistent with the number of points where this loop intersects with the discriminant surface. Besides,  $\lambda_1$  and  $\lambda_2$  become conjugate when

they are complex.

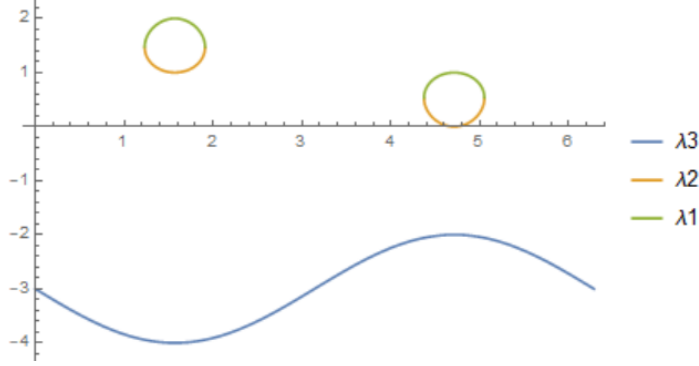


**Figure 22 Eigenvalues**

Take corresponding eigenvectors as the following

$$v_1 = \begin{pmatrix} \frac{1}{4}(\sqrt{-14 - 18 \cos 2t} \sec t + 2 \tan t) \\ 1 \\ 1 \end{pmatrix}$$

$$v_2 = \begin{pmatrix} \frac{1}{4}(-\sqrt{-14 - 18 \cos 2t} \sec t + 2 \tan t) \\ 1 \\ 1 \end{pmatrix}$$

$$v_3 = \begin{pmatrix} 0 \\ -1 \\ 1 \end{pmatrix}$$

$v_3$  is a constant vector, and thus has a trivial bundle. Using the method in section 4.1, we can obtain the evolutions of  $v_1$  and  $v_2$  by only calculating their first components.

Let

$$a(t) = |\sqrt{-14 - 18 \cos 2t}| \sec t$$

$$b(t) = 2 \tan t$$

Then, when  $v_2$  and  $v_3$  are real, they can be written as

$$v_1 = \begin{pmatrix} \frac{1}{4}(a(t) + b(t)) \\ 1 \\ 1 \end{pmatrix}$$

$$v_2 = \begin{pmatrix} \frac{1}{4}(-a(t) + b(t)) \\ 1 \\ 1 \end{pmatrix}$$

When  $v_2$  and  $v_3$  are complex, write

$$v_1 = \begin{pmatrix} \frac{1}{4}(a(t)i + b(t)) \\ 1 \\ 1 \end{pmatrix}$$

$$v_2 = \begin{pmatrix} \frac{1}{4}(-a(t)i + b(t)) \\ 1 \\ 1 \end{pmatrix}$$

The images of  $a(t)$  and  $b(t)$  are

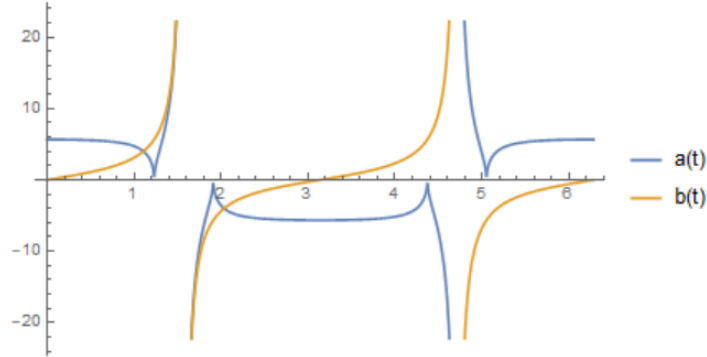


**Figure 23** The images of  $a(t)$  and  $b(t)$

Note that the first components of two eigenvectors have a discontinuous point respectively. Therefore, we can draw a conclusion that they change to the opposite direction after  $2\pi$ .

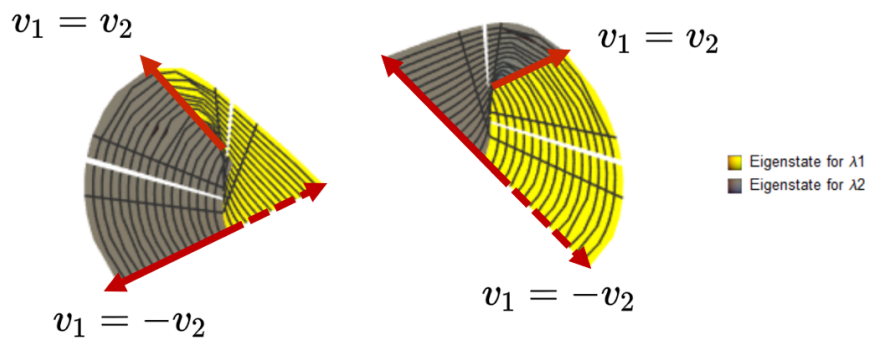


**Figure 24** Eigenvector bundles

Moreover, we can plot two segments of bundles where  $v_1$  and  $v_2$  are real. (see Figure 24) In each segment, two vectors with the same direction will rotate to opposite directions. In two complex regions, one is where the two eigenvectors are conjugate, and another one

is where  $v_1$  and  $-v_2$  are conjugate. Their evolution is similar to the two eigenvectors of the 2-band non-Hermitian case in section 3.2.

**Example 4.4** The fourth loop (see Figure 21(b)) is a more complicated but more interesting loop.

From the root structure, we can obtain the evolution of three eigenvectors directly in the segment where they are all real vectors. (see Figure 25) In this segment,  $v_2$  changes from  $v_2 = v_3$  at the left b to  $v_2 = v_1$  at the right b. Then,  $v_2$  keep conjugate with  $v_1$  and change to  $-v_3$  when returning to the left b. So, there are two nontrivial eigenvector bundles exchange with a trivial bundle along this loop.

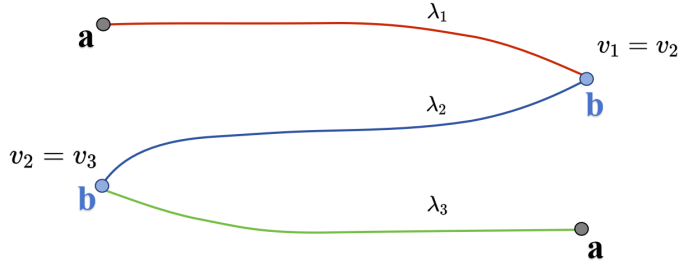


**Figure 25 Eigenvectors in real region**

**Example 4.5** The fifth loop (see Figure 21(c)) has 3 trivial bundles, although it intersects with the discriminant surface.

## 5. Further work

Aiming to make classification, we consider the Moduli space. For example, the Moduli space  $M_2$  of 2-band non-Hermitian Hamiltonian is  $S^1 \vee S^1 \vee S^{1[4]}$  and then we can obtain  $\pi_1(M_2)$ . For  $n \geq 3$ ,  $\pi_1(M_n)$  is non-Abelian<sup>[5]</sup> and much more complicated than  $M_2$ .

Additionally, since we hope to figure out the evolution of eigenvectors, we consider eigenvector bundles. If we see unit real vectors  $v$  and  $-v$  as two points, then the behavior along loops can be seen as principle  $S^0$ -bundles over  $S^1$ .

**Proposition 5.1** There are only two principle  $S^0$ -bundles over  $S^1$ . (see Cohen 2002, Theorem 2.7<sup>[6]</sup>)

- The trivial bundle

$$S^0 \hookrightarrow S^1 \times S^0 \longrightarrow S^1$$

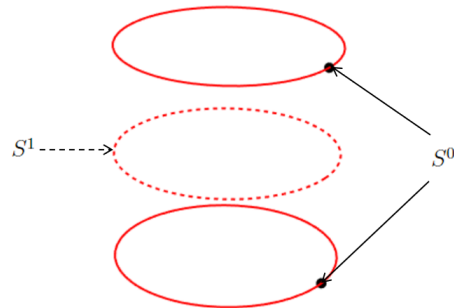


**Figure 26 Trivial bundle**

The total space  $S^1 \times S^0$  is disconnected. In Example 4.1,  $v_1$  cannot change to  $-v_1$  after  $2\pi$ . So, its bundle is trivial.

- The Hopf bundle

$$S^0 \hookrightarrow S^1 \longrightarrow S^1$$

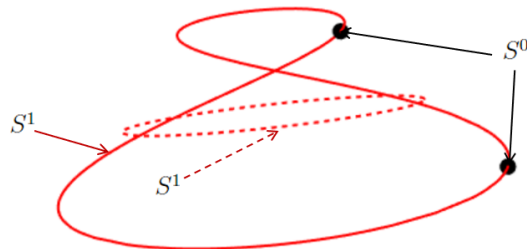


**Figure 27 Hopf bundle**

The total space  $S^1$  is connected and is isomorphic to the margin of a Möbius band. In Example 4.1,  $v_2$  and  $v_3$  change to  $-v_2$  and  $-v_3$  after  $2\pi$ . So, the corresponding two eigenvector bundles are Hopf bundles.

For the loop 1 and loop 3 we have calculated in section 4, they all have two Hopf bundles and one trivial bundle. However, the corresponding eigenvectors for Hopf bundles

are different. For loop 1,  $v_2$  and  $v_3$  generate Hopf bundles, while for loop 3,  $v_1$  and  $v_2$  generate Hopf bundles.

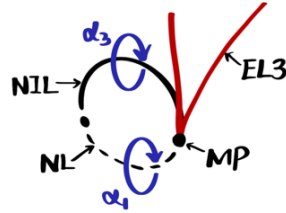


**Figure 28 Loop 1 and Loop 3**

However, only these two kinds of bundles is not enough to classify loops. In Example 4.2, all eigenvectors return to their initial direction. However, the bundles of  $v_2$  and  $v_3$  are non-trivial. Actually, loop 2 can be seen as two loop 1 connected.

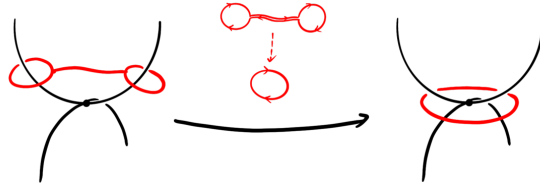


**Figure 29 Another way to obtain loop 2**

The two non-trivial bundles of loop 2 both are formed by two Hopf bundles. However, two Hopf bundles connected can be a trivial bundle. We need to consider the orientation to distinguish between two different situations in Figure 18.

Moreover,  $S^0$  is not enough for complex vectors. Additionally, in Example 4.4, the eigenvector bundles exchange. So, only consider bundles formed by one eigenvector is not enough. We need to find the relation between eigenvectors or their bundles.

## References

- [1] Hu, J., Zhang, RY., Wang, T. *et al.* Non-Hermitian swallowtail catastrophe revealing transitions among diverse topological singularities.[J] *Nat. Phys.* **19**, 1098-1103 (2023).
- [2] Jaap Top and Erik Weitenberg, *Resurfaced discriminant surfaces*[J], Eur. Math. Soc. Newslet. (2011), no. 79, 28-35.
- [3] Ross, E. Stratified Vector Bundles: Examples and Constructions[J/OL]. <https://doi.org/10.48550/arXiv.2303.04200>, (2023).
- [4] Jia, H., Zhang, RY., Hu, J. *et al.* Topological classification for intersection singularities of exceptional surfaces in pseudo-Hermitian systems.[J] *Commun Phys* **6**, 293 (2023).
- [5] Wu *et al.* Non-Abelian band topology in noninteracting metals[J] *Sci* **365**, 1273–1277 (2019).
- [6] Cohen, R. L. The Topology of Fiber Bundles Lecture Notes.[J/OL]. <http://math.stanford.edu/~ralph/fiber.pdf>, (2002).

# Appendix

Here is part of codes for calculation.

```

ClearAll["Global`*"]
 $\text{清除全部}$ 

(*2-band non-Hermitian case: Using sin,cos or tan to make components continuous*)

Plot[{ $\frac{\sin[\frac{-2t+3\pi}{4}]}{\text{Norm}[\sin[\frac{-2t+3\pi}{4}]]} * \frac{\sin[t] + \sqrt{-\cos[2t]}}{\text{Norm}[\{\sin[t] + \sqrt{-\cos[2t]}, -\cos[t]\}]}$ },
 $\frac{\sin[\frac{-2t+3\pi}{4}]}{\text{Norm}[\sin[\frac{-2t+3\pi}{4}]]} * \frac{\sqrt{\cos[2t]}}{\text{Norm}[\sqrt{\cos[2t]}]} * \frac{\sin[t]}{\text{Norm}[\{\sin[t] + \sqrt{-\cos[2t]}, -\cos[t]\}]}$ ,
 $-\frac{\sin[\frac{-2t+3\pi}{4}]}{\text{Norm}[\sin[\frac{-2t+3\pi}{4}]]} * \frac{\cos[t]}{\text{Norm}[\{\sin[t] + \sqrt{-\cos[2t]}, -\cos[t]\}]}$ ,
 $\frac{\sin[\frac{-2t+3\pi}{4}]}{\text{Norm}[\sin[\frac{-2t+3\pi}{4}]]} * \frac{\sqrt{\cos[2t]}}{\text{Norm}[\{\sin[t] + \sqrt{-\cos[2t]}, -\cos[t]\}]}$ },
{t, 0, 2 * Pi}, PlotStyle -> {RGBColor[0, 0, .9], RGBColor[0, .3, .9], Orange,
 $\dots$   $\text{绘图样式}$   $\text{RGB颜色}$   $\text{RGB颜色}$   $\text{橙色}$ 
{Dashed, RGBColor[0, .3, .9]}}, PlotLegends -> {"a(t)+c(t) when v+ is real",
 $\text{虚线}$   $\text{RGB颜色}$   $\text{绘图图例}$ 
"a(t) when v+ is complex", "b(t)", "c(t) when v+ is complex"}]

(*How to plot the discriminant surface*)

H[f1_, f2_, f3_] :=  $\begin{pmatrix} 1 & f1 & f2 \\ -f1 & -1 & f3 \\ -f2 & f3 & -1 \end{pmatrix}$ ;
s = 3;

plotH = ContourPlot3D[Discriminant[CharacteristicPolynomial[H[f1, f2, f3], \omega], \omega] == 0,
 $\text{三维等高线}$   $\text{判别式}$   $\text{(广义)特征多项式}$ 
{f1, -s, s}, {f2, -s, s}, {f3, -s, s}, AxesLabel -> Automatic,
 $\text{坐标轴标签}$   $\text{自动}$ 
Mesh -> None, ContourStyle -> Opacity[0.6]];
 $\text{网格}$   $\text{无}$   $\text{等高线样式}$   $\text{不透明度}$ 

(*Plot the ELs*)
 $\text{绘图}$ 

plotEL = ParametricPlot3D[{{- $\frac{\sqrt{36 + 27 f3^2 - \frac{\sqrt{f3^2 (-4 + 9 f3^2)^3}}{f3^2}}}{3 \sqrt{6}}$ }},
 $\text{绘制三维参数图}$ 
 $\frac{1}{-4 - 27 f3^2} \left( -2 \sqrt{6} f3 \sqrt{36 + 27 f3^2 - \frac{\sqrt{f3^2 (-4 + 9 f3^2)^3}}{f3^2}} - 3 \sqrt{\frac{3}{2}} f3^3 \right)$ 

```

$$\begin{aligned}
& \left. \left\{ \sqrt{\frac{36 + 27 f3^2 - \frac{\sqrt{f3^2 (-4 + 9 f3^2)^3}}{f3^2}}{f3^2}} + \frac{f3 \left( 36 + 27 f3^2 - \frac{\sqrt{f3^2 (-4 + 9 f3^2)^3}}{f3^2} \right)^{3/2}}{6 \sqrt{6}}, f3 \right\}, \right. \\
& \left. \left\{ \frac{\sqrt{\frac{36 + 27 f3^2 - \frac{\sqrt{f3^2 (-4 + 9 f3^2)^3}}{f3^2}}{f3^2}}}{3 \sqrt{6}}, \frac{1}{-4 - 27 f3^2} \right. \right. \\
& \left. \left. \left( 2 \sqrt{6} f3 \sqrt{\frac{36 + 27 f3^2 - \frac{\sqrt{f3^2 (-4 + 9 f3^2)^3}}{f3^2}}{f3^2}} + \right. \right. \right. \\
& \left. \left. \left. 3 \sqrt{\frac{3}{2} f3^3} \sqrt{\frac{36 + 27 f3^2 - \frac{\sqrt{f3^2 (-4 + 9 f3^2)^3}}{f3^2}}{f3^2}} - \frac{f3 \left( 36 + 27 f3^2 - \frac{\sqrt{f3^2 (-4 + 9 f3^2)^3}}{f3^2} \right)^{3/2}}{6 \sqrt{6}} \right) \right\}, \right. \\
& \left. f3 \right\}, \left\{ -\frac{\sqrt{\frac{36 + 27 f3^2 + \frac{\sqrt{f3^2 (-4 + 9 f3^2)^3}}{f3^2}}{f3^2}}}{3 \sqrt{6}}, \frac{1}{-4 - 27 f3^2} \right. \\
& \left. \left( -2 \sqrt{6} f3 \sqrt{\frac{36 + 27 f3^2 + \frac{\sqrt{f3^2 (-4 + 9 f3^2)^3}}{f3^2}}{f3^2}} - 3 \sqrt{\frac{3}{2} f3^3} \right. \right. \\
& \left. \left. \left( \sqrt{\frac{36 + 27 f3^2 + \frac{\sqrt{f3^2 (-4 + 9 f3^2)^3}}{f3^2}}{f3^2}} + \frac{f3 \left( 36 + 27 f3^2 + \frac{\sqrt{f3^2 (-4 + 9 f3^2)^3}}{f3^2} \right)^{3/2}}{6 \sqrt{6}} \right) \right\}, f3 \right\},
\end{aligned}$$

$$\left\{ \frac{\sqrt{\frac{36 + 27 f3^2 + \sqrt{\frac{f3^2 (-4 + 9 f3^2)^3}{f3^2}}}{3 \sqrt{6}}}, \frac{1}{-4 - 27 f3^2} \right. \\ \left. \left( 2 \sqrt{6} f3 \sqrt{\frac{36 + 27 f3^2 + \sqrt{\frac{f3^2 (-4 + 9 f3^2)^3}{f3^2}}}{f3^2}} + \right. \right. \\ \left. \left. 3 \sqrt{\frac{3}{2}} f3^3 \sqrt{\frac{36 + 27 f3^2 + \sqrt{\frac{f3^2 (-4 + 9 f3^2)^3}{f3^2}}}{f3^2}} - \right. \right. \\ \left. \left. f3 \left( \frac{36 + 27 f3^2 + \sqrt{\frac{f3^2 (-4 + 9 f3^2)^3}{f3^2}}}{f3^2} \right)^{3/2} \right) \right. \\ \left. \left. , f3 \right\} \right\}, \{f3, -s, s\}, \text{PlotStyle} \rightarrow \text{Red} \right];$$

[绘图样式] [红色]

(\*How to obtain eigenvalues and eigenvectors\*)

`Eigenvalues[H[\frac{1}{2}Cos[t], \frac{1}{2}Sin[t], \theta]]`

[特征值] [余弦] [正弦]

`Eigenvectors[H[\frac{1}{2}Cos[t], \frac{1}{2}Sin[t], \theta]]`

[特征向量] [余弦] [正弦]

(\*How to plot a vector bundle\*)

`ParametricPlot3D[\{\{\frac{1}{2}Cos[t], \frac{1}{2}Sin[t], \theta\} +`

[绘制三维参数图] [余弦] [正弦]

$\frac{\text{Sin}[t]}{\text{Norm}[\text{Sin}[t]]} * \frac{v}{\text{Norm}[\{-2 \csc[t] + \sqrt{3} \csc[t], \csc[t] \sec[t] - \tan[t], 1\}]}$

$\{\left(\csc[t] \sec[t] - \tan[t]\right) \sin[t + \frac{\pi}{4}] + \left(-2 \csc[t] + \sqrt{3} \csc[t]\right) \cos[t + \frac{\pi}{4}],$

$-\sin[t + \frac{\pi}{4}] \left(-2 \csc[t] + \sqrt{3} \csc[t]\right) + \cos[t + \frac{\pi}{4}] \left(\csc[t] \sec[t] - \tan[t], 1\right)\}\},$

`{t, \theta, 2 \pi}, {v, \theta, .3}, Boxed \rightarrow False, Axes \rightarrow False,`

[边界框] [假] [坐标轴] [假]

`PlotLegends \rightarrow {"Eigenstate for \lambda2"},`

[绘图的图例]

`PlotStyle \rightarrow LightGreen]`

[绘图样式] [浅绿]

## Acknowledgements

Grateful thanks to Professor Zhu for his guidance and assistance. Also, thanks to my partners Zhou Fang and Wenhui Yang for their related work. The discussion with them gave me inspiration and gains. Finally, thanks to Pingyao Feng for her the preliminary work.